17th International Conference on Greenhouse Gas Control Technologies, GHGT-17

20th -24th October 2024 Calgary, Canada

# Fracture Networks Imaging in $CO_2$ Injection Zones in IBDP Site: An Unsupervised Machine Learning Application with Multiple Datasets

Abhash Kumar[b,c], William Harbert[b,c], Evgeniy Myshakin[b,c], Guoxiang Liu[c]*, Hema Siriwardane[a],

[a]*National Energy Technology Laboratory, 3610 Collins Ferry Road, Morgantown, WV 26505, USA*
[b]*NETL Support Contractor, 626 Cochran Mill Road, Pittsburgh, PA 15236, USA*
[c]*National Energy Technology Laboratory, 626 Cochran Mill Road, Pittsburgh, PA 15236, USA*

**Abstract**

Storing carbon dioxide ($CO_2$) in geological formations is a technology reducing anthropogenic $CO_2$ emissions continues to grow into the atmosphere. This technology plays a crucial role in reducing greenhouse gas emissions and mitigating the impacts of anthropogenic climate change. As we delve into the intricacies of $CO_2$ injection operations, it becomes evident that a comprehensive understanding of fracture networks within the reservoir and its immediate vicinity of injection wells are essential for ensuring the operational efficiency and permanent retention. In this context, the integration of machine learning (ML) techniques, especially unsupervised machine learnings emerge as a transformative tool for advancing our understanding of $CO_2$ injection into reservoirs that could potentially contribute to optimizing injection strategies and reservoir management, ultimately bolstering the efficacy and sustainability of $CO_2$ sequestration operations and deployment. This paper demonstrates the fracture network imaging by using machine learning techniques based on multiple datasets of microseimic and injection records.

*Keywords: $CO_2$ Injection; $CO_2$ Storage, IBDP; Machine Learning;Multiple Datasets; Fracture Network; Microseismic Data; Geomechanics*

## 1. Introduction

Capturing carbon dioxide ($CO_2$) and storing (CCS) into geological reservoirs is one of the piloted practices for greenhouse gas reduction. These operations have gained considerable traction in the last decade as a viable option to reduce the long-term environmental footprint. However, monitoring the storage reservoir to ensure safe and long-term storage of $CO_2$ for de-risk operations and storage management is undergoing dynamic shifts, expanding opportunities for implementing innovative techniques and applications, especially for the commercial-scale deployment. Our ongoing efforts in the SMART (Science-informed Machine Learning for Accelerating Real-time Decisions in Subsurface Applications) Initiative Phase II project involve harnessing the potential of data assimilation and ML algorithms to quantify the spatial distribution of fracture networks at the Illinois Basin Decatur Project (IBDP) site.

* Corresponding author. Tel.: +1-412-386-7386, *E-mail* address: guoxiang.liu@netl.doe.gov

In the paper, we utilized a microseismic catalog recorded between November 2011 and July 2018 at the $CO_2$ injection site in Decatur, Illinois that consisted of 5,397 microseismic events. The injection period was identified 19 discrete time windows throughout three-year injection period that are marked by an extended period of bottom hole pressure changes from monitoring. We used the beginning and ending times of these windows to create corresponding subsets of microseismic catalogs based on event origin times. To facilitate the imaging of the fracture network associated with individual time windows, we first leveraged the potential of hydraulic diffusivity that is a critical concept for microseismic triggering front identification. In such way, there was a total of 53 microseismic triggering fronts was identified throughout the event catalog and then used them to create an input dataset for a suite of unsupervised ML algorithms. Leveraging ML-based clustering algorithms enabled us to autonomously analyze large volumes of microseismic data from individual triggering fronts. We were able to quantify more than 100 discrete clusters of microseismic events likely associated with reactivation of pre-existing fractures or induced fractures due to $CO_2$ injection. This fracture network mapping brings valuable insights to geomechanical response of an engineered system to fluid injection operations, monitoring designs, risk assessments, and reservoir management. We also created pseudo-logs of microseismic attributes (moment magnitude, b-value, and event count) by means of vertical moving-average sampling of microseismic data at the sampling interval matching that of the geomechanical well logs. This is helpful to create an ML-based predictive model to quantify the probability of occurrence of microseismic events of certain magnitude depending upon the geomechanical properties of rock layers. This physics-based ML approach will help enhance the understanding of subsurface reservoirs behaviour under $CO_2$ injection that could be utilized for optimized well scheme, injection strategies, and operational efficiency for de-risked geological storage. Furthermore, this methodology proves to be highly applicable in reservoir characterization analyses for other fluid injection activities related to hydrocarbon explorations and/or geothermal resources extensively [1, 2, 3, 4, 10, 11, 12, 13, 14]. As stated above, the current SMART Initiative phase II demonstrations include the use of all accessible datasets from the first-of-its-kind Illinois Basin – Decatur Project (IBDP). The major goal of the phase is to mature the technologies from proof-of-concept prototypes to demonstration of their capabilities and values for the element/segment of CCS project regarding to subsurface storage from phase I. The IBDP is an integrated industrial carbon capture and storage system from source to reservoir. The project stored $CO_2$ from ADM's ethanol fermentation plant [5, 6, 7, 8, 9]. In the study, an innovative method comprising multi-levelled/tiered analysis has been developed to leverage advanced machine learning (ML) techniques to process passive seismic monitoring data acquired over the three-year injection period in the Illinois Basin for potential fracture/fault analysis [5, 8, 9]. This use case is aimed at contributing to the risk assessment and monitoring design for carbon storage. For IBDP demonstration, a three-year injection period of data was analysed for identifying multiple distinct time windows in this paper by associated with microseismic data records [5].

## 2. Methodology

A multi-tiered, data-driven approach was developed by coupling all available measurement data to visualize fracture networks. The datasets can be included measurements from drilling, log and core testing, injection, and downhole pressure measurements, and five vertical pressure monitoring gauges, providing a wealth of detail on the fracture networks. A fracture network encompasses natural fractures, induced/hydraulic fractures, and the dynamic response of such fractures, culminating in a comprehensive understanding of this system. Before of the wide spectrum of resolutions and scales of the datasets, the fracture network was mapped into 19 distinct time windows over a three-year injection period by analyzing pumping data, which included $CO_2$ injection and bottom-hole pressure. We compartmentalized passive seismic data (microseismic) into these time windows, which is like industry practices of compartmentalizing microseismic data into separate stages for high-pressure fluid injection activities (i.e., induced fracturing). In each of these time windows, we estimated the b-value of the associated microseismic population. Then further used event occurrence time and distance from the treatment well to identify the distinct triggering front of microseismicity that are likely associated with pre-existing fractures and faults within the reservoir. Seismogenic b-value and diffusivity analysis were applied to identify triggered fronts for further clustering, fracture plane, and 3D fracture distribution analysis. Moreover, we leveraged the potential of several unsupervised ML algorithms to identify the spatial clusters of microseismic events within each triggering front of individual time windows by following the workflow in Fig. 1. Furthermore, such ML techniques were implemented determining the best fitting surface for each spatial cluster of microseismicity to infer the directional and spatial distributions of fractures as shown in Fig. 1. Moreover, well logs including imaging log and core datasets from the drilling and test in the laboratory are applied to

verify what the results produced from microseismic data and pumping data. Such multi-datasets provide another angle of the cross-checking observations to the outcomes for uncertainty reduction.

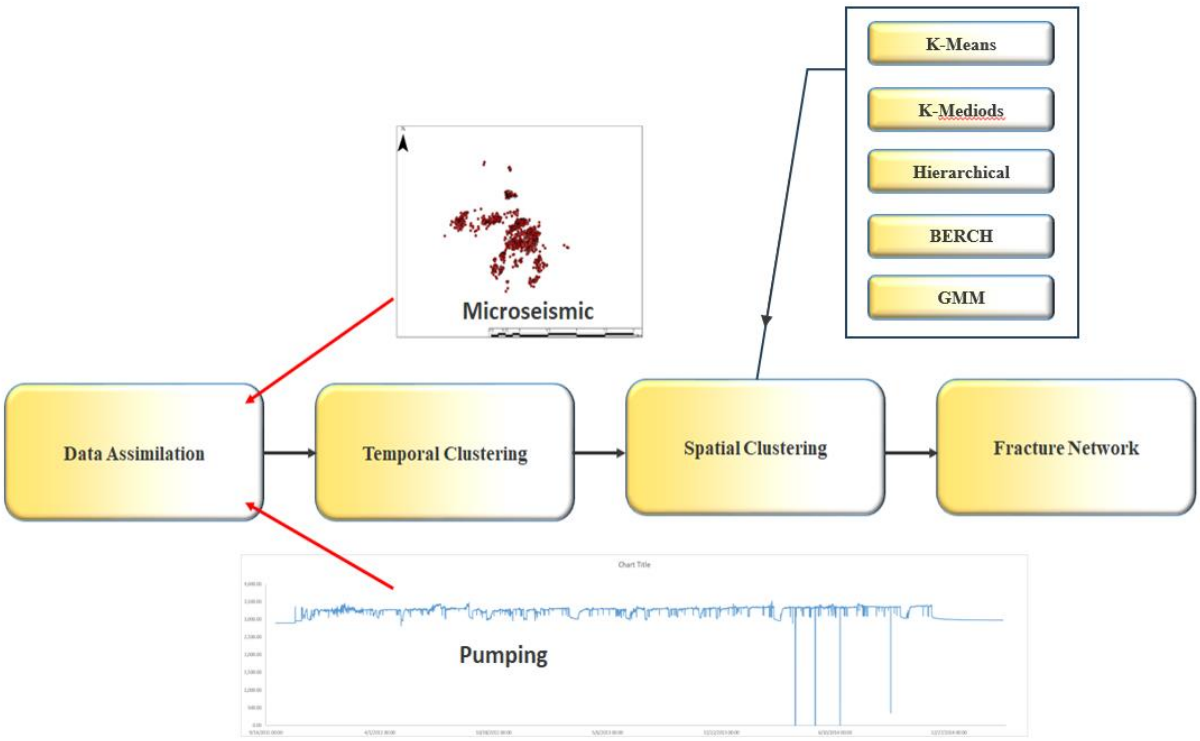


Fig. 1. Workflow for the study with Microseicmic data and pumping data coupling [4]

### *2.1. IBDP Datasets*

Based on the collaboration and data availability $CO_2$ injection pilot in the field, Illinois Basin – Decatur Project (IBDP) has been selected as the demonstration use case along with SMART Initiative investigation. The project was cumulatively injected one million metric tons of anthropogenic $CO_2$ into a saline reservoir, the Mt. Simon Sandstone, in Decatur, Illinois in Fig. 2. Operational $CO_2$ injection began on November 17, 2011, at a nominal rate of 1,000 metric tons per day. After three years of operations, the injection goal was met in November 2014. Capacity, injectivity, and containment potential have met and/or exceeded pre-injection expectations [4, 8, 9]. The Mt. Simon Sandstone of the Illinois Basin contains a locally significant saline aquifer, which is ideal for $CO_2$ storage with adequate capacity and injectivity and is overlain by the impermeable Eau Claire Formation as a caprock. The Mt. Simon Sandstone represents the primary $CO_2$ storage resource in the Illinois Basin and the Midwest region and is more than 457 meters (1,500 feet) thick at the IBDP site. The upper portion was deposited in a tidally influenced system, while the lower 183 meters (600 feet) is an arkosic sandstone that was deposited in a braided river/alluvial fan system. The lower Mt. Simon Sandstone is the principal target for storage, in part because the dissolution of feldspar grains has created good secondary porosity. The Eau Claire Formation is the primary confining layer, or seal, and is 212 meters (695 feet) thick. The lower Eau Claire consists of shale and the upper unit consists of low-permeability limestone and siltstone [4, 7, 8, 9].

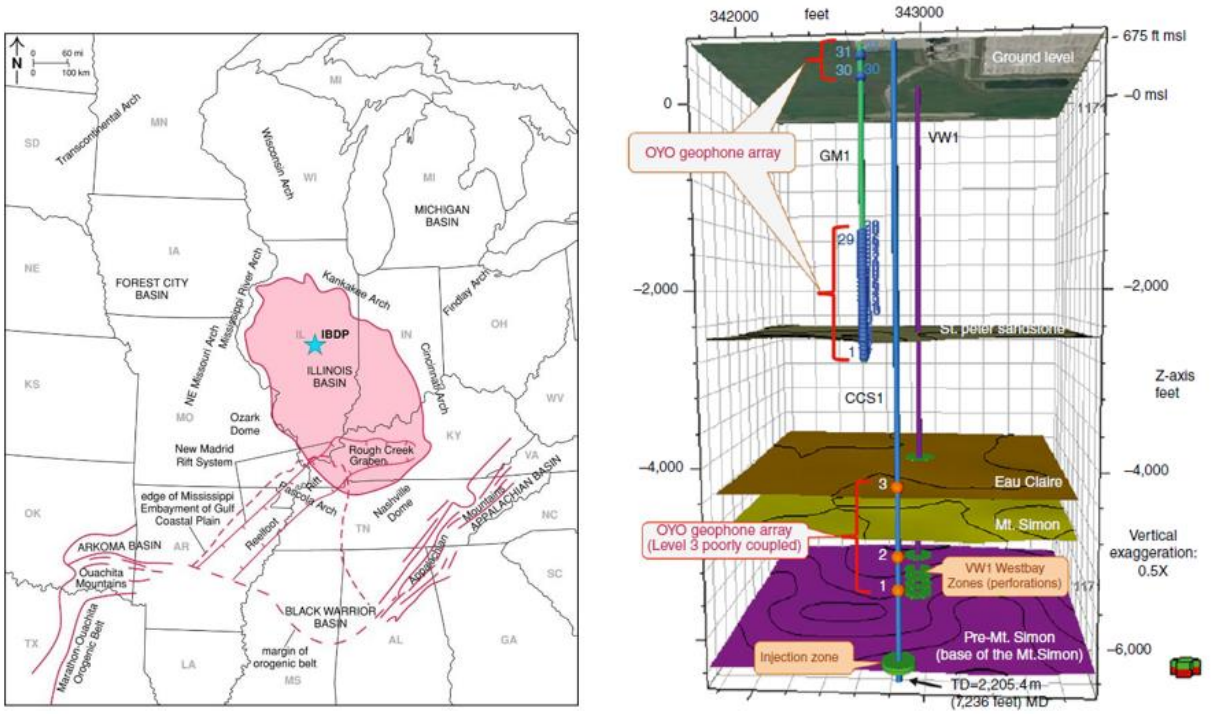


Fig. 2. IBDP Project location (left) and vertical formations along the wells CCS1, GM1, and VW1 (right) [4]

IBDP was the world's first bioenergy carbon capture and storage (BECCS) project, an integrated industrial CCS system from source to reservoir. The project used $CO_2$ from ADM's ethanol fermentation process. Operations consisted of a compression/dehydration facility, a delivery pipeline, one injection well, one deep observation/verification well, a geophysical test well, and an integrated environmental monitoring system, all developed on the ADM-owned site [4, 7, 8, 9]. The real-time acquisition and control (RTAC) and Well Watcher Connect systems were specifically created to provide continuous subsurface project data, such as wellhead pressure and temperature, downhole pressure and temperature, and annulus pressure, which is critical to operational monitoring. This data was recorded, archived, and continuously accessible. The software recorded and formatted pressure, temperature, annulus pressure, and injected volumes as required for permit reporting [4]. Site operations at IBDP were administered through the RTAC software. $CO_2$ from ethanol production had been injected through one well (CCS1) three perforation zones of CCS1, which are the upper injection zone, the middle injection zone, and the lower injection zone as shown in Fig. 2 [4, 8]. In addition, there is one deep monitoring well (VW1) with six multi-depth sensors in a deep monitor well VW1, which are WB1, WB2, WB3, WB4, WB5, and WB6 for more collection (NETL 2023). In this study, we performed data assimilation of microseismic catalog, bottom hole pressure, and $CO_2$ injection rate for the IBDP site. The microseismic data was recorded by three downhole arrays deployed respectively in the injection well (CCS1), geophysical monitoring well (GM1) and verification well (VW2) in Fig. 2.

### *2.2. Geophysical Analysis*

Geophysical analysis engaged in the case study includes Seismogenic b-value analysis and diffusivity analysis to quantify fracture network.

#### ***Seismogenic b-value Analysis***

The seismogenic b-value describes the frequency-magnitude distribution of a microseismic catalog. It represents the logarithmic relationship between the number of earthquakes and their magnitudes given by the Gutenberg-Richter

relationship. The details reported in the publications [11, 15, 16, 17].

$$log(N) = a - b * M$$

where, N is the number of earthquakes with a magnitude greater than or equal to M, a is a constant term related to the total number of earthquakes in the catalog, and b is the b-value, representing the slope of the earthquake frequency versus magnitude plot above the magnitude of completeness. The range of b-value has a critical geomechanical significance in terms of stress conditions and fault behavior. A higher b-value (greater than 1) indicates a larger proportion of small-magnitude earthquakes relative to larger ones with tensile stress condition. This can suggest a more fractured or weaker crust, where earthquakes occur more frequently but with lower magnitudes. It may imply a more active fault system or a higher likelihood of small to moderate seismic activity. Conversely, a lower b-value (less than 1) suggests a relatively lower occurrence of small-magnitude earthquakes compared to larger events with compressive stress regime. This can indicate a more stable or locked fault system, where larger earthquakes are more prevalent. A temporal change in the b-value can provide further geomechanical insights. An increase in the b-value over time might indicate stress accumulation or the growth of the fracture network, potentially leading to larger earthquakes in the future. Conversely, a decrease in the b-value could suggest stress relaxation or a contraction of the fracture network. We estimated b-value for each time window to quantify its temporal changes in Fig. 3. Majority of the time windows have b-value close to 1, indicating shear stress regime and strike-slip faulting. Two windows, 10 and 18 show b-values more than 1.2, indicating tensile stress regime or normal faulting. Similarly, two other windows (13 and 15) showing b-value less than 0.8, which is indicative of compressional regime.

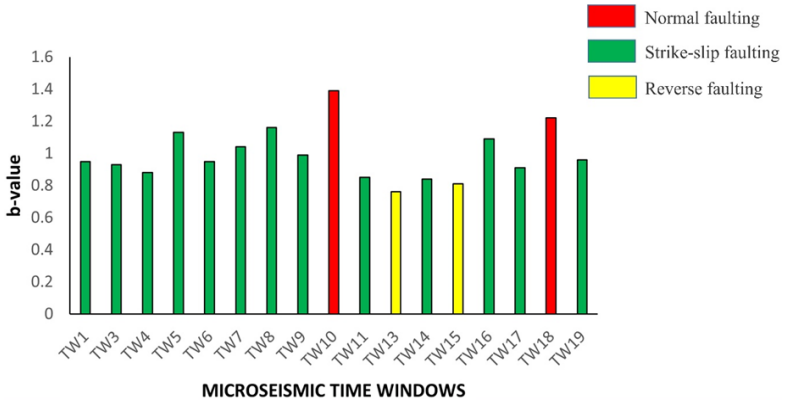


Fig. 3. Bar plot showing variations in b-value estimates for 19 different time windows [4]

### *Diffusivity Analysis*

Hydraulic diffusivity is a parameter that represents the ability of a fluid to propagate through a porous medium under the influence of hydraulic gradients. It combines the properties of fluid conductivity and storage capacity within the medium. In the context of microseismic triggering fronts and hydraulic fracture networks, hydraulic diffusivity plays a significant role. It provides insights into the ability of the fluid to spread and migrate through the porous medium, influencing the propagation of hydraulic fractures and the formation of fracture networks. As microseismic events are triggered by the propagation of fluid and associated pore pressure perturbation through the rock mass, which is guided by diffusivity, hence in general terms hydraulic diffusivity is a critical factor that affects the microseismic triggering and propagation of these fractures. Higher hydraulic diffusivity indicates greater fluid mobility, facilitating the expansion of hydraulic fractures and increasing the likelihood of microseismic events. Therefore, a higher hydraulic diffusivity allows for more extensive fracture networks with increased connectivity, enhancing the effectiveness of $CO_2$ storage and their preferential flow paths. For the homogeneous and isotropic rock mass, hydraulic diffusivity could be estimated as the best fitting parabola to the microseismic cloud in the cross plot of relative distance (between injection well and individual microseismic event) and relative origin time (difference between event origin time and beginning time of corresponding pumping time window) and given by the following expression [4, 5, 16,

17]:

$$r_t(t) = \sqrt{4\pi D_{tf} t}$$

Where, $D_{tf}$ is the triggering front diffusivity, r is the distance of microseismic event from the treatment well and t is the elapsed time between the start of fluid injection and the microseismic event. For each of r-t plots in each time window, and we found discrete bands of microseismicity on the r-t plot in Fig. 4. Interestingly, events in these bands are triggered at the same time even though their effective distances from the injection well are different. This suggests a very effective fluid or pressure connectivity among fractures or faults associated with microseismic events for these individual bands of triggering fronts.

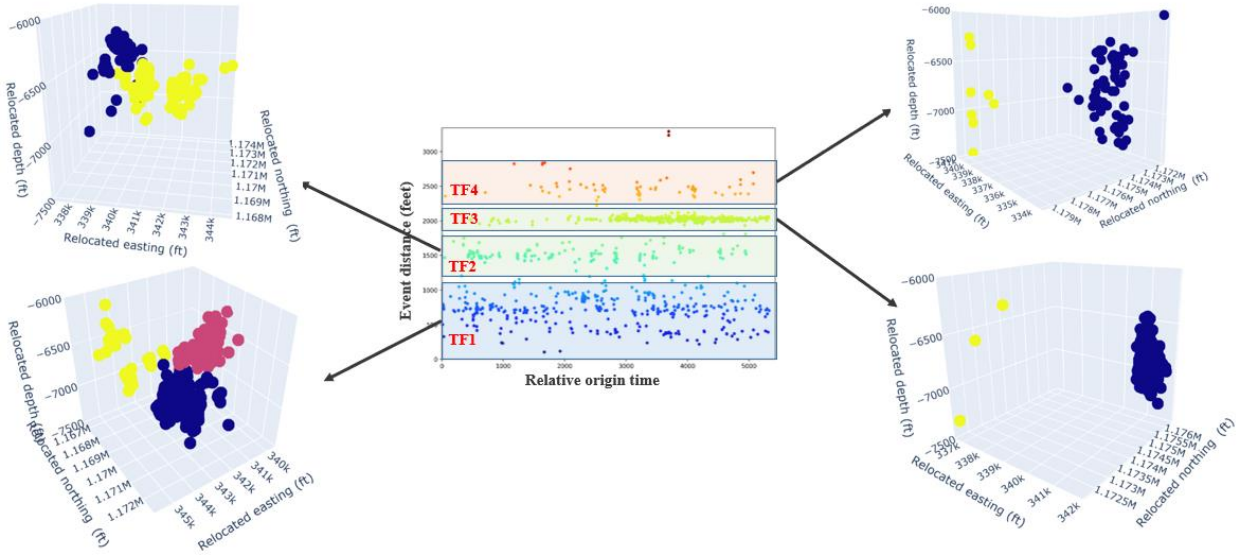


Fig. 4. Event clustering using unsupervised machine learning listed in Fig. 1 within each triggering front of time window 17 (as an example for plot illustration). Data points are color coded to differentiate among individual clusters [4].

## 3. Results and Discussions

Based upon the distribution of microseismic triggering fronts in each time window, we obtained multiple subsets of events. Although there is multiple spatial grouping of events within each microseismic triggering front, we are unable to visually specify them to separate clusters. In the absence of class label for specific cluster for individual microseismic events, we leveraged the potential of unsupervised machine learning algorithms to find meaningful spatial clusters in the microseismic cloud. We tested K-Means, Hierarchical, BIRCH, and GMM clustering techniques that are good at uncovering hidden patterns in the unclassified data. We leveraged the potential of these ML algorithms to identify spatial clusters of events within each triggering front for individual time windows. It allowed us to find natural spatial grouping in microseismic events that were originally unlabelled within each triggering front as shown in Fig. 5.

To obtain best fitting fracture plane for individual microseismic clusters, we tested two different algorithms. At first, we tried to fit plane in the least square sense that minimize that minimizes the perpendicular distances between the points and the plane. However, the least square surface seems to be not an actual representation of the fracture plane as majority of the microseismic events are either above or below the plane for respective clusters. This is in stark contrast of the actual fracture plane for which most of the microseismic events should be coplanar. Therefore, we approximated the fracture planes as 2-sigma standard deviation ellipsoids, which closely represents the spread and orientation of a 3D distribution of data points in Fig. 5. It captures the spatial spread of the points along different axes and allows for an understanding of the variability within the dataset. The size and orientation of the ellipsoid provide

insights into the major and minor axes of the data distribution. As can be seen in Fig. 5, most of the microseismic events are in-plane to the standard deviation ellipsoid. We decide to use 2-sigma ellipsoid to capture 95% of the events in the respective microseismic cloud. As an outcome of our ML implementation, we obtained a complex network of interconnected fractures around the injection well in Fig. 6. This dense network of fractures could be used to infer possible $CO_2$ flow paths at a finer scale in the reservoir.

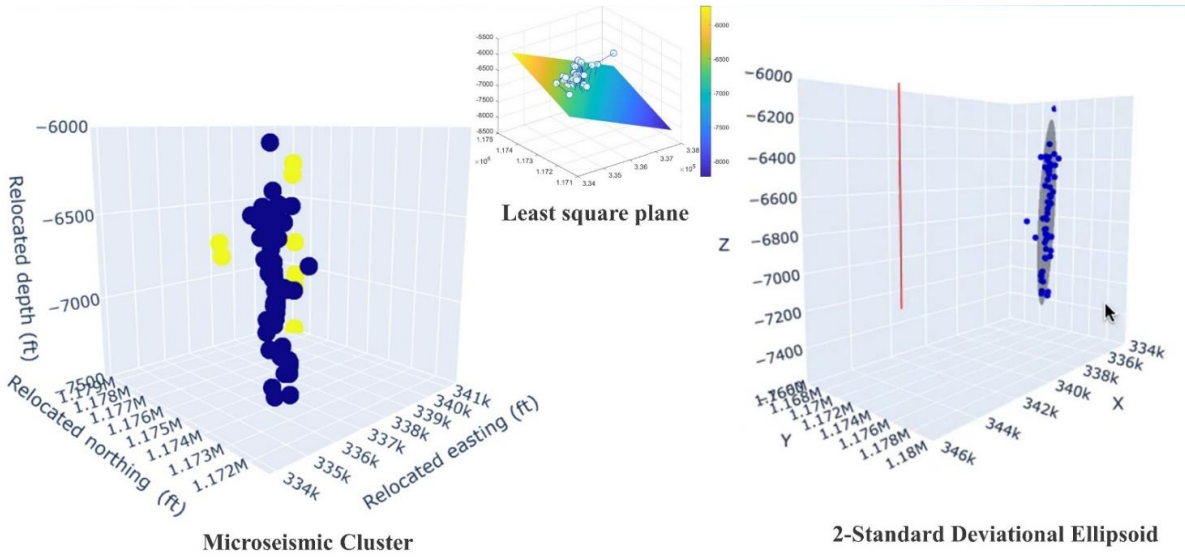


Fig. 5. Example of the fracture quantification test methods of least square plane and 2-standard deviation ellipsoid [4]

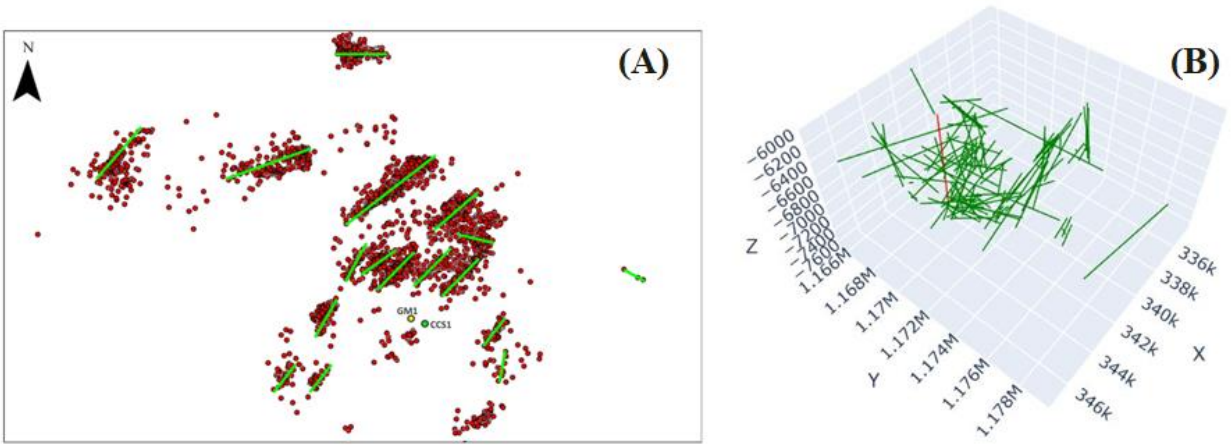


Fig. 6. Fracture network comparison. Left panel shows the fault plane solution (green lines) as reported earlier by Bauer et al. [8]. Right panel shows the fracture network orientation (green lines) as determined using the unsupervised ML algorithm in the current study [4].

## 4. Remarks and Future Work

The study with IBDP case demonstrated a multi-tier analysis of microseismic and injection datasets, each evaluated at its own resolution and scale, to achieve a comprehensive understanding of fracture networks around the wellbore at the IBDP site. By assimilating data from multiple sources, the study successfully analyzed and quantified fracture behavior induced by $CO_2$ injection. The workflow integrated several key components: 1) Microseismic Time Window Analysis: Quantification of microseismic activity throughout the injection period. 2) Physics-Based Machine Learning: Application of machine learning algorithms to classify and quantify microseismic event clusters. 3) Spatial

Mapping of Fracture Networks: Reservoir-scale fracture network mapping and volume analysis. 4) These analyses provided valuable insights into the fracture network induced by $CO_2$ injection, highlighting the benefits of such data-driven workflows for field data processing and interpretation. The results are critical for designing monitoring systems, assessing risks, and optimizing injection strategies for effective carbon storage. The understanding of fracture networks can also inform decision-making in broader applications beyond carbon storage, such as: 1) Completion and fracture design in unconventional resources. 2) Mitigation of frac-hits and wellbore protection. 3) Production performance analysis and re-fracturing/stimulation planning.

Based on what the current study, further integration of multi-level analyses is planned to develop a more comprehensive understanding of fracture networks. This will incorporate additional datasets, including more surrounding well logs, imaging logs, core tests, and pressure measurements from six monitoring well gauges. The workflow, implemented using Python libraries, has been integrated into the SMART Initiative Visualization and Decision Support Platform to support future carbon storage deployments. This ongoing effort aims to enhance fracture network modeling and decision-making capabilities for carbon storage and other subsurface applications.

## Acknowledgements

This material is based upon work supported by the U.S. Department of Energy, National Energy Technology Laboratory. Authors also thank to Sherilyn Williams-Stroud for her contribution of data sharing.



## References

[1] Ringrose, P (2010), Modeling CO2 Injection and Storage, IEA-GHG CCS Summer School, Svalbard, 22-28 August, accessed at https://ieaghg.org/docs/General_Docs/Summer_School/Philip_Ringrose_Storage_3.pdf

[2] Mishra, S, Schuetter, J., Datta-Gupta, A., and Bromhal, G, (2021), Robust Data-Driven Machine Learning Models for Subsurface Applications: Are We There Yet?, J. Petroleum Tech. (March), 15-21.

[3] Liu, G, Kumar, A, Beautz, S, Mark-Moser, M, Cunha, L, Gonzalez, D, Nguyen, J, Qawasmeh, S, Vaughn, D, Yang, H, Chen, J, Crandall, D, Mckoy, M, Hakala, A, Machine Learning Powered Multi-Tier of Fracture Imaging: A Case Study, Geothermal Rising Conference, October 27-30, 2024, Waikoloa, HI

[4] Liu, G, Kumar, A, Harbert, W, Siriwardane, H, Crandall, D, Bromhal, G, and Cunha, L, "Machine Learning Application for CCUS Carbon Storage: Fracture Analysis and Mapping in the Illinois Basin." Paper presented at the SPE Annual Technical Conference and Exhibition, San Antonio, Texas, USA, October 2023. doi: https://doi.org/10.2118/214996-MS

[5] Um, ES, Alumbaugh, D, Lin, S. (2022), Real-time deep-learning inversion of seismic full waveform data for CO2 saturation and uncertainty in geological carbon storage monitoring, Geophysical Prospecting. (25 March 22) https://doi.org/10.1111/1365-2478.13197

[6] Bromhal, G, Mishra, S, Guthrie, G, Alumbaugh, D, Crandall, D, White, J, Williams-Stroud, S, Azzolina, N, McGuire, T, Pawar, R, Schuetter, J, Morris, J, Butler, S, Viswanathan, H, Carr, T, The SMART Initiative: Applying Machine Learning to Enable Efficient and Effective Real-Time Decisions for Geological Carbon Storage Operations (December 7, 2022). 16th International Conference on Greenhouse Gas Control Technologies GHGT-16 23-27th October 2022, Lyon, France, Available at SSRN: https://ssrn.com/abstract=4296267 or http://dx.doi.org/10.2139/ssrn.4296267.

[7] National Energy Technology Laboratory (NETL), Illinois Basin – Decatur Project (IBDP) | netl.doe.gov, access on Dec. 1, 2024

[8] Bauer, R; Carney, M; Finley, R; Overview of microseismic response to CO2 injection into the Mt. Simon saline reservoir at the Illinois Basin-Decatur Project, International Journal of Greenhouse Gas Control, Volume 54, Part 1, 2016, Pages 378-388, ISSN 1750-5836, https://doi.org/10.1016/j.ijggc.2015.12.015.

[9] Finley, RJ An overview of the Illinois Basin — Decatur Project. Greenh. Gases Sci. Technol. 4, 571–579 (2014).

[10] Klenner, R, Liu, G, Stephenson, H, Murrell, G, Iyer, N, Virani, N, and Charuvaka, A, 5 Sept 2018. Characterization of Fracture-Driven Interference and the Application of Machine Learning to Improve Operational Efficiency. Society of Petroleum Engineers Liquids-Rich

Basin Conference. https://doi.org/10.2118/191789-MS
[11] Liu, G, Stephenson, H, Shahkarami, A, Murrell, G, Klenner, R, Iyer, N, Barr, N, and Nurali V, Accelerated Completion Optimization with Uncertainty Reduction Through Coupled Data and Physics Based Hybrid Models. Paper presented at the SPE Oklahoma City Oil and Gas Symposium, Oklahoma City, Oklahoma, USA, April 2019. doi: https://doi.org/10.2118/195238-MS
[12] Kumar, A, Shih, CY, Liu, G, Holcomb, P, Zhao, S, Hammack, R, Ilconich, J, and Bromhal, G, Machine Learning Applications for a Qualitative Evaluation of the Fracture Network in the Wolfcamp Shale Using Tracer and Completion Data. Paper presented at the SPE/AAPG/SEG Unconventional Resources Technology Conference, Houston, Texas, USA, July 2021. doi: https://doi.org/10.15530/urtec-2021-5159
[13] Kumar, A, HFTS-1 Fracture Network Quantification; SMART -001-2022; NETL Technical Report Series; U.S. Department of Energy, National Energy Technology Laboratory: Pittsburgh, PA, 2022
[14] Liu, G; Kumar, A; Zhao, S; Shih, C; Vasylkivska, V; Holcomb, P; Hammack, R; Illconich, J; Bromhal, G; Multi-Level of Fracture Network Imaging: A HFTS Use Case and Knowledge Transferring, Paper presented at the SPE/AAPG/SEG Unconventional Resources Technology Conference, Houston, Texas, USA, June 2022. Paper Number: URTEC-3723466-MS, https://doi.org/10.15530/urtec-2022-3723466
[15] NETL, Internal Summary Report of Available Data Sets, Physics-Based Models and Machine Learning Tools, 2022
[16] Rothert, E, Shapiro, SA, Buske, S, and Bohnhoff, M (2003). Mutual relationship between microseismicity and seismic reflectivity: case study at the German continental deep drilling site (KTB). Geophys. Res. Lett. 30:1893. doi: 10.1029/2003GL017848
[17] Shapiro, S; Rothert, E; Rath, V; Rindschwentner, J; Characterization of fluid transport properties of reservoirs using induced microseismicity. Geophysics 2002; 67 (1): 212–220. doi: https://doi.org/10.1190/1.1451597